

# Self-Healing of Trotter Error in Digital Adiabatic State Preparation

Lucas K. Kovalsky<sup>1,\*</sup> Fernando A. Calderon-Vargas<sup>1</sup> Matthew D. Grace<sup>1</sup> Alicia B. Magann<sup>2</sup>

James B. Larsen<sup>2,3</sup> Andrew D. Baczewski<sup>2,†</sup> and Mohan Sarovar<sup>1,‡</sup>

<sup>1</sup>Quantum Algorithms and Applications Collaboratory, Sandia National Laboratories, Livermore, California 94550, USA

<sup>2</sup>Quantum Algorithms and Applications Collaboratory, Sandia National Laboratories, Albuquerque, New Mexico 87185, USA

<sup>3</sup>Department of Mathematics, Brigham Young University, Provo, Utah 84602, USA

(Received 2 October 2022; revised 18 April 2023; accepted 29 June 2023; published 7 August 2023)

Adiabatic time evolution can be used to prepare a complicated quantum many-body state from one that is easier to synthesize and Trotterization can be used to implement such an evolution digitally. The complex interplay between nonadiabaticity and digitization influences the infidelity of this process. We prove that the first-order Trotterization of a complete adiabatic evolution has a cumulative infidelity that scales as  $\mathcal{O}(T^{-2}\delta t^2)$  instead of  $\mathcal{O}(T^2\delta t^2)$  expected from general Trotter error bounds, where  $\delta t$  is the time step and  $T$  is the total time. This result suggests a self-healing mechanism and explains why, despite increasing  $T$ , infidelities for fixed- $\delta t$  digitized evolutions still decrease for a wide variety of Hamiltonians. It also establishes a correspondence between the quantum approximate optimization algorithm and digitized quantum annealing.

DOI: 10.1103/PhysRevLett.131.060602

Preparing the ground state of a quantum many-body Hamiltonian is generically difficult [1–3]. Nevertheless, because we frequently observe systems near their ground state in nature, we expect to be able to efficiently prepare these states in laboratories or on quantum computers for a wide range of physical Hamiltonians [4–8]. One approach to ground state preparation is through an adiabatic evolution that interpolates between a Hamiltonian with an easy-to-prepare ground state ( $H_1$ ) and a Hamiltonian with the target ground state ( $H_2$ ). This has applications in quantum computation [9,10], linear algebra [11–13], optimization [14], and simulation [15–17]. Realizing these applications requires an understanding of the sources of error in adiabatic state preparation (ASP).

The total error is often quantified as the infidelity  $\mathcal{I}$  of the prepared state relative to the ideal target state. An ever-present contribution to  $\mathcal{I}$  is due to the fact that such an evolution cannot proceed infinitely slowly in practice [18,19]. Digitizing the evolution into  $r$  time steps via Trotterization [20,21], as would be necessary on a gate-based quantum computer [22,23], introduces a second influence on  $\mathcal{I}$  due to the fact that we cannot exactly represent the ideal continuous-time dynamics. This Letter explores the interplay between these effects.

We show that certain errors cancel out over the course of a *complete* adiabatic evolution from  $H_1$  to  $H_2$  requiring time  $T$ . One should expect digitization to degrade  $\mathcal{I}$  for larger  $T$  with a fixed time step  $\delta t = T/r$ , i.e., more time steps lead to more accumulation of errors. Indeed, a generic upper bound on  $\mathcal{I}$  for first-order Trotterization suggests that its error scales as  $\mathcal{O}(T^2\delta t^2)$ . This would mean that  $\delta t$  needs to decrease to realize a fixed  $\mathcal{I}$  as  $T$  increases. However,

numerical results suggest that  $\mathcal{I}$  *decreases* with increasing  $T$ , even for fixed  $\delta t$ .

We present a less generic upper bound on  $\mathcal{I}$  in Theorem 1, similar to one recently proved for time-independent Hamiltonians by Layden [24]. This bound relies on adiabaticity, but not on the evolution being

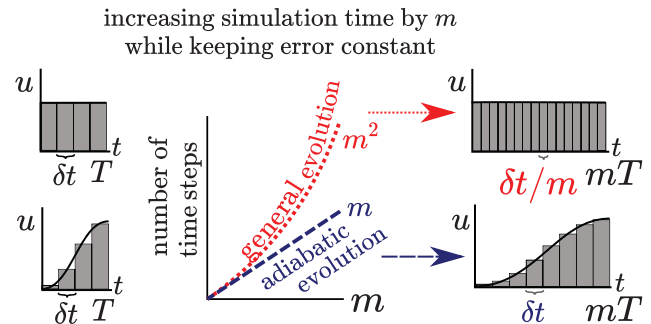


FIG. 1. Consider a Hamiltonian with two terms,  $H[u(t)] = [1 - u(t)]H_1 + u(t)H_2$ . A time evolution from  $t = 0$  to  $t = T$  can be broken into steps of size  $\delta t$  through first-order Trotterization (left). For a general evolution of this sort, previously established bounds suggest that cumulative infidelity should grow with total time  $T$  for fixed  $\delta t$ . Then, scaling  $T$  by  $m$  should require dividing  $\delta t$  by  $m$  to preserve a fixed infidelity (top right). However, for an adiabatic evolution from  $u(0) = 0$  to  $u(T) = 1$ , we show that cumulative infidelity actually scales as  $\mathcal{O}(T^{-2}\delta t^2) + \mathcal{O}(T^{-2})$  (Theorem 2). This allows us to keep  $\delta t$  fixed if we scale  $T$  by  $m$ , to achieve a fixed or decreasing infidelity, consistent with the continuous-time limit (bottom right). Thus, the total number of time steps will be at least quadratically lower than expected (center).

complete. While it improves the scaling with  $T$ , it does not explain reductions in  $\mathcal{I}$  with increasing  $T$  for fixed  $\delta t$ .

However, Theorem 2 gives conditions under which  $\mathcal{I}$  instead *improves* with the duration of the evolution, consistent with numerics. This bound relies on both adiabaticity and the evolution being complete. Critically, it allows for further Trotterization of  $H_1$  and  $H_2$ , as might be required in applications like quantum simulation. It also does not rely on the ordering of the Trotterization. Figure 1 summarizes the primary consequence of Theorem 2.

The crossover between the bounds in Theorems 1 and 2 suggest a *self-healing* mechanism for complete adiabatic evolutions. There is a sense in which  $\mathcal{I}$  gets worse before it gets better, and this is supported by numerical results. We will also show that this explains a relationship between Trotterized quantum annealing and the quantum approximate optimization algorithm (QAOA) [25–27].

We begin by considering an adiabatic evolution generated by a time-dependent Hamiltonian,  $H[u(t)] = [1 - u(t)]H_1 + u(t)H_2$ , for  $u(t) \in [0, 1]$ , where  $u(t)$  is 0 at  $t = 0$  and 1 at  $t = T$ . The unitary associated with the continuous-time dynamics is  $U(t) = \mathcal{T} \exp\{-i \int_0^t H[u(t')] dt'\}$ , where  $\mathcal{T}$  is the time-ordering operator.  $U(t)$  is approximated by digitizing the time evolution with first-order Trotterization [20–22,28,29]. We will be particularly interested in the Trotterization of the complete adiabatic evolution,

$$U(T) \approx U^{(1)}(T) = \prod_{k=1}^r \prod_{i=1}^2 U_i((k-1)\delta t, k\delta t), \quad (1)$$

where  $U_1((k-1)\delta t, k\delta t) = e^{-iH_1 \int_{(k-1)\delta t}^{k\delta t} dt' [1-u(t')]}$  and  $U_2((k-1)\delta t, k\delta t) = e^{-iH_2 \int_{(k-1)\delta t}^{k\delta t} dt' u(t')}$  [30].

The error incurred by splitting the exponential this way is typically called the Trotter error and scales as  $\|U(T) - U^{(1)}(T)\| = \mathcal{O}(T\delta t \| [H_1, H_2] \|)$ , where  $\|\cdot\|$  is the operator norm. Note that  $T\delta t = r\delta t^2 = T^2/r$ , and this scaling represents the leading-order contribution to the error in  $\delta t$ . It can be derived by bounding the error in a single time step and applying the triangle inequality to aggregate the error over all  $r$  steps [20,31]. When  $\mathcal{I}$  is defined as  $\mathcal{I}(T) \equiv 1 - |\langle \psi | U^\dagger(\infty) U^{(1)}(T) | \psi \rangle|$  [32], then it accounts for infidelity from both digitization and non-adiabaticity. Specifically,  $\mathcal{I}$  is upper bounded by the squared sum of the Trotter error  $\|U(T) - U^{(1)}(T)\|$  and an energy gap-dependent  $\mathcal{O}(T^{-1})$  term accounting for nonadiabaticity (see Lemma 4 in the Supplemental Material [33]). Theorems 1 and 2 improve on this bound for less generic adiabatic evolutions.

That this is possible is motivated by numerical investigations. Figure 2 shows  $\mathcal{I}$  as a function of  $\delta t$  for a simple two-level system described in terms of Pauli matrices. For this example,  $H_1 = X$ ,  $H_2 = Z$ , and the schedule  $u(t) = t/T$  is a linear ramp. While this is the simplest possible

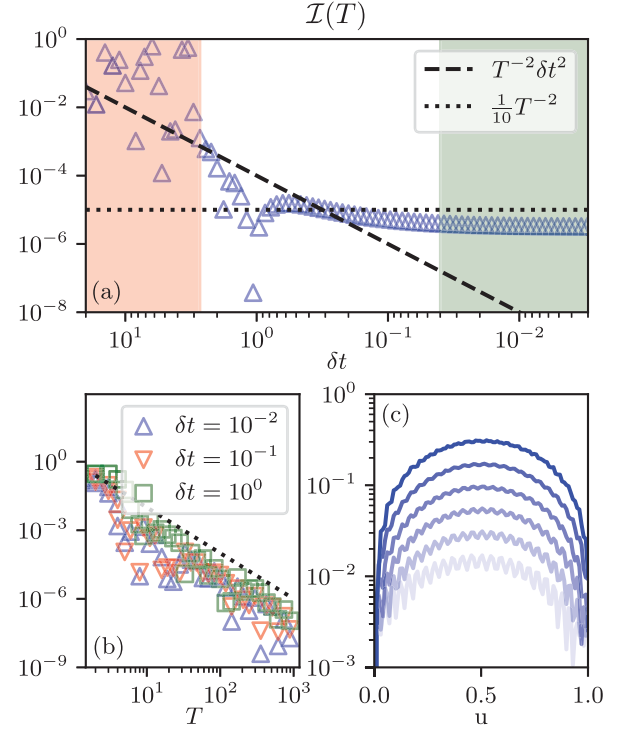


FIG. 2. Infidelity of digitized ASP for a two-level system. (a) Scaling of  $\mathcal{I}(T)$  with Trotter time step size  $\delta t$ , for fixed evolution time  $T = 100$ . The dashed and dotted lines show scalings that dominate the upper bound on  $\mathcal{I}(T)$  for different values of  $\delta t$ . (b) Scaling of  $\mathcal{I}(T)$  with  $T$  for different values of  $\delta t \leq 1$ . The dashed line shows  $T^{-2}$  scaling, rather than a generic  $\sim T^2$  scaling that might be expected due to digitization error. (c) Intermediate infidelities as a function of  $u$ , with increasing  $\delta t$  corresponding to increasing opacity. The larger the value of  $\delta t$ , the higher the peak of intermediate infidelity at  $u = 1/2$ . A self-healing mechanism for complete adiabatic evolutions is evident, as the infidelity comes back down for  $u = 1$ .

example, the phenomenology that it captures generalizes to more complicated choices for  $H_1$  and  $H_2$ , some of which are considered in the Supplemental Material [33]. In the red-shaded region of Fig. 2,  $\delta t \|H(t)\| \in \Omega(1)$  and the Trotter product formula is nonconvergent in this region. We do not expect predictable scaling of error with  $\delta t$  in this region and focus on the behavior in the white and green-shaded regions.

We draw attention to two interesting features in Fig. 2. First, the observed scaling of  $\mathcal{I}$  is much more favorable than the scaling suggested by the generic  $\mathcal{O}(T^2\delta t^2)$  upper bound given above. We instead see a  $\mathcal{O}(T^{-2}\delta t^2)$  scaling, which is completely inconsistent with the expectation that error should increase with  $T$ . This inconsistency is due to the use of the triangle inequality in deriving the generic Trotter error bound, which neglects error cancellation effects evident in Fig. 2(c). The second feature is that  $\mathcal{I}$  asymptotes to a  $\delta t$  independent quantity as  $\delta t \rightarrow 0$  in Fig. 2(a). In this green-shaded region, the digitization error

is smaller than the finite- $T$  nonadiabaticity error, and thus  $\mathcal{I}$  is independent of  $\delta t$  and consistent with  $\mathcal{O}(T^{-2})$  bounds on the continuous-time adiabatic evolution [49,50].

Our first result is an improved upper bound on the Trotter error associated with the approximation in Eq. (1).

*Theorem 1 (informal).*—Given a gapped Hamiltonian  $H[u(t)] = [1 - u(t)]H_1 + u(t)H_2$  and a unitary  $U(T) = \mathcal{T}e^{-i\int_0^T H[u(t')]dt'}$ , where  $u(t) = s(t/T)$  and  $s: [0, 1] \rightarrow [0, 1]$ , if this unitary is first-order Trotterized into  $H_1$  and  $H_2$  terms with  $r$  time steps of size  $\delta t$ , as in Eq. (1), then as  $T \rightarrow \infty$ ,  $\mathcal{I}(T)$  is upper bounded by  $\min\{1, C_2 T^2 \delta t^2, (C_1 \delta t + C_3 T \delta t^2)^2\} + \mathcal{O}(\delta t) + \mathcal{O}(T^{-2})$ .

The formal version of Theorem 1 defines the coefficients  $C_i$  that determine the relative magnitudes of the contributions to the error [33]. The coefficients of the nonadiabatic  $\mathcal{O}(\delta t)$  and  $\mathcal{O}(T^{-2})$  terms depend on the energy gap [49,50]. We note that Theorem 1 only applies to two-term first-order Trotterization, which means that  $U_1$  and  $U_2$  cannot be further Trotterized.

Theorem 1 tightens the generic  $\mathcal{O}(T^2 \delta t^2)$  scaling of  $\mathcal{I}(T)$  to  $\mathcal{O}(T^2 \delta t^4)$  and  $\mathcal{O}(\delta t^2)$  in some regimes dependent on the  $C_i$  coefficients. The proof involves combining the first-order Trotter error from subsequent time steps into cumulative second-order Trotter error, similar to a recent bound for evolution under a time-independent Hamiltonian [24]. The main ingredients are bounds on the time-dependent first- and second-order Trotter expansion errors that do not require treating discretization error explicitly, in contrast to prior approaches, and they sidestep explicit Magnus expansion [51–53]. As in the time-independent case, the two contributions  $C_1 \delta t + C_3 T \delta t^2$  dominate in different parameter regimes.  $\mathcal{O}(T \delta t^2)$  scaling occurs when the evolution is long enough that the end points are insignificant, while  $T$ -independent  $\mathcal{O}(\delta t)$  scaling occurs when the evolution is short enough that the end points dominate [24].

While Theorem 1 introduces a scaling independent of  $T$  in the short-time regime unlike generic bounds, it does not capture the decrease in  $\mathcal{I}$  with increasing  $T$  for fixed- $\delta t$  evolutions, evident in Fig. 2(b). This is because the proof technique relies on adiabaticity (i.e., that  $u'$  and  $u''$  go to 0 and the Hamiltonian is gapped), but it does not rely on the fact that the adiabatic evolution is complete (i.e., that  $u$  goes from 0 to 1). Our second result shows that accounting for this leads to a bound with the anticipated behavior.

*Theorem 2.*—Given a gapped Hamiltonian  $H[u(t)] = [1 - u(t)]H_1 + u(t)H_2$  and a unitary  $U(T) = \mathcal{T}e^{-i\int_0^T H[u(t')]dt'}$ , where  $u(t) = s(t/T)$  is smooth and  $s: [0, 1] \rightarrow [0, 1]$ , if  $U(T)$  is first-order Trotterized with fixed time steps  $\delta t \in \mathcal{O}(\min_r \|H[u(t)]\|^{-1})$ , then as  $T \rightarrow \infty$  with  $u(0) \rightarrow 0$  and  $u(T) \rightarrow 1$  the final state infidelity is bounded by  $\mathcal{O}(T^{-2} \delta t^2) + \mathcal{O}(T^{-2})$ . Moreover, initially at a given fixed  $t/T \ll 1$ , state infidelity increases as  $\mathcal{O}(t^2 \delta t^2)$ .

The  $\mathcal{O}(T^{-2})$  term is again due to energy gap-dependent nonadiabaticity error associated with finite- $T$  evolution.

Note that the short-time  $\mathcal{O}(t^2 \delta t^2)$  bound matches the generic  $\mathcal{O}(T^2 \delta t^2)$  Trotter error bound.

The proof technique [33] involves analyzing the coefficients of the discretized time evolution of the ground state in the adiabatic basis using first-order time-dependent perturbation theory. This approach reveals that the leading-order error from Trotterization is due to an off-diagonal harmonic perturbation with amplitude  $\mathcal{O}(\delta t)$ . While its amplitude is independent of  $T$ , its frequency scales as  $T^{-1}$ . Thus, as  $T$  increases, this low-frequency perturbation becomes increasingly off resonant and it induces transitions out of the ground state with a probability  $\mathcal{O}(T^{-2} \delta t^2)$ , i.e., similar to the Lorentzian tail that appears in the solution of the Rabi problem [54].

Theorem 2's scaling holds for all gapped Hamiltonians, even with simple linear control ramps  $u(t)$ , as corroborated by numerical results [33]. We believe this generality explains the widespread inverse-in- $T$  scaling reported elsewhere [27,55].

Figure 3 illustrates the error bounds in Theorems 1 and 2 for the same simple two-level system studied in Fig. 2. To illustrate the bounds in Theorem 1, it is necessary to consider incomplete adiabatic evolutions, as to avoid the superior scaling that complete evolutions achieve according to Theorem 2. Thus, we examine  $\mathcal{I}(t)$  for  $t \leq T$ , in which the states relative to which infidelities are evaluated are the instantaneous ground states of  $H[u(t)]$ .

For the  $t \ll T$  evolution,  $\mathcal{I}$  initially scales as the generic bound  $\mathcal{O}(T^2 \delta t^2)$  (dashed line) in Theorem 1 and then crosses over to  $\mathcal{O}(\delta t)$  scaling (solid line). The constant coefficients in Theorem 1 dictate the size of the  $\mathcal{O}(\delta t)$ -scaling region, which is due to a cross-term involving both Trotter error and nonadiabatic error, and we see that this region dominates the  $t = 0.95T$  scaling for most of the relevant  $\delta t$  values [33]. The  $t = T$  curve achieves  $\mathcal{O}(T^{-2} \delta t^2)$  scaling because it is a complete evolution. As in Fig. 2, all three curves plateau at small  $\delta t$  (large  $r$ ) once the digitization error is dominated by the finite- $T$  nonadiabaticity error. We briefly note that the size of the  $\mathcal{O}(T^2 \delta t^2)$ -scaling region compared to  $\mathcal{O}(\delta t)$  can be changed if variable time steps are used [33].

Figure 3 also reveals an interesting crossover in the dependence of  $\mathcal{I}(t)$  on  $\delta t$  as  $t \rightarrow T$ . This is evident in the white region, in which the error bounds given by Theorems 1 and 2 are  $\mathcal{O}(T^2 \delta t^2)$  and  $\mathcal{O}(T^{-2} \delta t^2)$ , respectively. The  $T$ -dependent part of the error can be written as  $\mathcal{O}(T^\gamma \delta t^2)$ , where  $\gamma$  transitions from 2 to  $-2$  as  $t \rightarrow T$ . As this limit is approached, the upper bound in Theorem 1 becomes looser and looser as the scaling transitions to the tighter upper bound in Theorem 2. It appears that the prefactor of the  $\mathcal{O}(T^\gamma \delta t^2)$  term remains relatively constant during this transition, and so the different  $T$  behavior is apparent by the shifted dashed curves in Fig. 3 as its power changes. For  $t = T$ , Theorem 2's bound becomes valid and

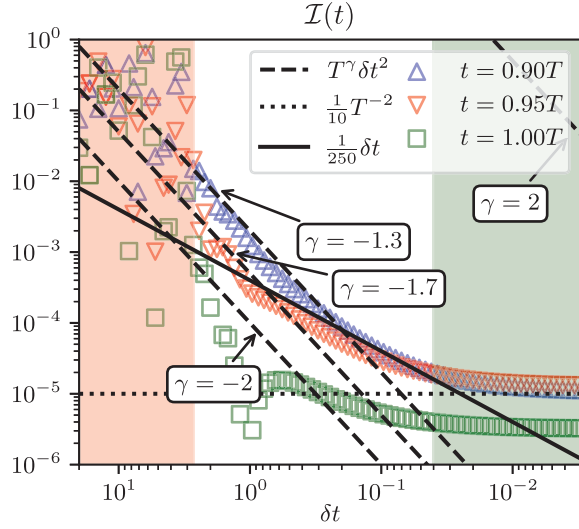


FIG. 3. Infidelity of digitized ASP for the same two-level system as in Fig. 2, but including intermediate evolutions  $U(t)$  for  $t \leq T$ .  $T = 100$  is fixed for all curves. Here  $\mathcal{I}$  considers the target state as the instantaneous ground state of  $H[u(t)]$  for the indicated values of  $t$ . The dashed and dotted lines show various scalings with  $\delta t$  and illustrate how the infidelity transitions from being dependent ( $\sim \delta t^2 T^2$ ) to inversely dependent ( $\sim T^{-2} \delta t^2$ ) on total time  $T$  as the evolution is completed.

$\mathcal{I}(t = T)$  decreases with  $T$  as  $\mathcal{O}(T^{-2} \delta t^2)$  for all relevant values of  $\delta t$ , as seen in Fig. 2(b).

Moreover, the transition from the initial  $\mathcal{O}(t^2 \delta t^2)$  scaling to the  $\mathcal{O}(T^{-2} \delta t^2)$  cumulative scaling implies a cancellation of errors incurred at intermediate times, evident in Fig. 2(c). We find this  $\mathcal{O}(t^2 \delta t^2)$  upper bound to be tight and that increasing ground state infidelity at intermediate times is reversed as  $t \rightarrow T$  after traversing the system's avoided crossing [33]. We do not prove the mechanism of the reversal, but the same phenomenon can be observed in more complex systems, where transitions to many excited states at intermediate times are reversed as  $t \rightarrow T$  [33]. This remarkable property of self-healing digitized adiabatic evolutions has been empirically observed, but had otherwise defied explanation [56,57].

This begs the question of how self-healing impacts higher-order Trotterization for adiabatic evolutions and resource requirements for ASP [33]. A  $p$ th-order generalization of Theorem 2 will still include a  $\delta t$ -independent  $\mathcal{O}(T^{-2})$  term, and the interplay of this diabatic error with improved  $\mathcal{O}(\delta t^p)$  digitization error requires further study. Our analysis also implies reductions in circuit depths for Trotterized ASP relative to generic bounds, with potentially significant consequences for resource estimates of ASP. However, the optimal approach to ground state preparation is likely to be problem dependent and a comparison of Trotterized ASP to alternatives [58–62] is a topic for future work.

In the context of optimization algorithms, our results establish a bijective correspondence between QAOA and

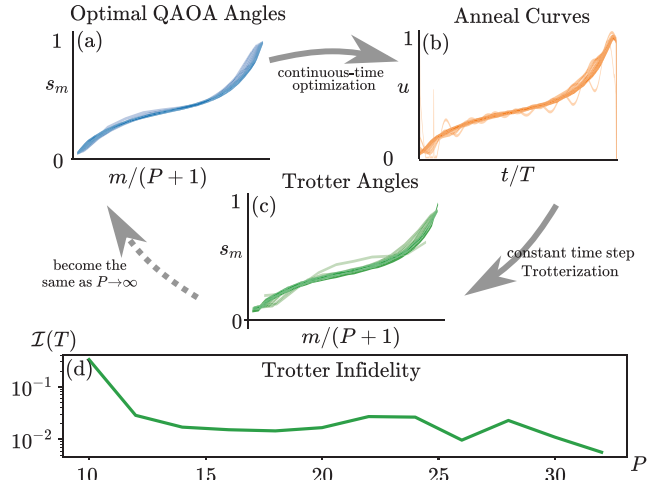


FIG. 4. Correspondence between QAOA and digitized quantum annealing. We consider a three-regular Ising model (MAXCUT) on  $N = 8$  qubits with periodic boundary conditions.  $s_m = \gamma_m / (\gamma_m + \beta_m)$ , where  $m \in [1, \dots, P]$  and  $\gamma_m$  ( $\beta_m$ ) are the  $m$ th QAOA angle corresponding to  $H_p$  ( $H_d$ ). (a) QAOA curves found for  $P = \{10, \dots, 32\}$  layers by bootstrapped seeding [63–65] from smaller  $P$  solutions (darker curves correspond to larger  $P$ ). (b) Optimal anneal curves found by seeding from the corresponding QAOA curves in (a). (c) Constant time step Trotterization of these anneal curves. (d) The infidelity with the ground state of  $H_p$  after evolution under the digitized annealing schedule. The decrease in infidelity demonstrates an instance when QAOA optimal angles can be considered to be proximal to a *constant nonvanishing*  $\delta t$  Trotterization of a universal family of anneal curves. This correspondence becomes exact as  $P \rightarrow \infty$  [33].

digitized quantum annealing [27,55]. As in Fig. 4, it is often possible to find an injective correspondence between a set of optimal angles for QAOA and a Trotterization of an optimized quasiadiabatic (or annealing) evolution between the driver ( $H_d$ ) and problem ( $H_p$ ) Hamiltonians. But justification for the surjective correspondence (QAOA angles from Trotterizing a given quasiadiabatic evolution) has remained elusive.

This is because, for a given set of  $P$  pairs of optimal QAOA angles [Fig. 4(a)], the corresponding continuous anneal control curve often has a similar total integrated time  $T$  [Fig. 4(b)]. This forces the time step of the QAOA to scale as  $\delta t \propto T/P$  when viewed as a Trotterization. Since  $P$  is generally found to be proportional to  $T$  in unrestricted QAOA, this becomes a fixed- $\delta t$  Trotterization. Such a Trotterization has been phenomenologically found to be the best discretization to match the oscillating curves of the adiabatic anneal, whose period scales as the ( $T$ -independent) energy gap [55]. Prior efforts were unable to prove the surjective correspondence between Figs. 4(a) and 4(c) because generic bounds suggest that error increases with  $T$  for fixed  $\delta t$ .

Here we have shown that, for the broad class of Hamiltonians that satisfy Theorem 2,  $\mathcal{I}$  is constant or

decreasing with fixed  $\delta t$  and increasing  $T$ . This facilitates proving the final relationship between Figs. 4(c) and 4(a), producing a fully bijective relationship between optimal QAOA angles and continuous anneal curves. Trotterization of these curves with  $\delta t = T/P$  produces angles [Fig. 4(c)] that, as  $P \rightarrow \infty$ , approach the original QAOA angles and evolve the initial state to the ground state with increasing fidelity [Fig. 4(d)].

Thus, at sufficiently large depth, QAOA can become a fixed- $\delta t$  digitization of an underlying set of quantum annealing curves, a limit that differs from the  $\delta t \rightarrow 0$  digitization of the adiabatic limit traditionally considered [66]. These annealing curves approach a single asymptotic curve as the total integrated time goes to infinity. This correspondence allows for high-depth QAOA instances to be seeded by interpolating low-depth instances [27,55,63–65] that converge quickly to the high-depth instance’s minimum. Theorem 2 justifies this widely used “bootstrap” procedure.

Based on prior Trotter bounds, it might have been expected that digitization error would dominate the cumulative infidelity of digitized ASP with increasing  $T$ . For a fixed  $\delta t$ , more time steps should lead to more error. However, thanks to a self-healing property of complete adiabatic evolutions, this is not the case. We have applied this to establish a correspondence between QAOA and digitized quantum annealing, but future work remains in exploring the mechanism of the self-healing property and consequences for other quantum algorithms that rely on ASP.

We acknowledge useful conversations with Jonathan Wurtz and Tameem Albash about portions of this work. We are also grateful to the anonymous referees whose thorough comments greatly improved its presentation. This material is based upon work supported by the U.S. Department of Energy, Office of Science, Office of Advanced Scientific Computing Research, under the Quantum Computing Application Teams (QCAT) and Accelerated Research in Quantum Computing (ARQC) programs, the National Nuclear Security Administration’s Advanced Simulation and Computing program, and the National Science Foundation under Grant No. NSF PHY-1748958. A. D. B., A. B. M., and J. B. L. acknowledge support from the Sandia National Laboratories Truman Fellowship Program, which is funded by the Laboratory Directed Research and Development (LDRD) program. Sandia National Laboratories is a multimission laboratory managed and operated by National Technology & Engineering Solutions of Sandia, LLC, a wholly owned subsidiary of Honeywell International Inc., for the U.S. Department of Energy’s National Nuclear Security Administration under Award No. DE-NA0003525. This Letter describes objective technical results and analysis. Any subjective views or opinions that might be expressed in the Letter do not necessarily represent the views of the U.S. Department of Energy or the U.S. Government.

\*lkocia@sandia.gov

†adbacze@sandia.gov

‡mnsarov@sandia.gov

- [1] A. Kitaev, A. Shen, and M. Vyalyi, *Classical and Quantum Computation* (American Mathematical Society, Providence, 2002), Vol. 47.
- [2] J. Kempe, A. Kitaev, and O. Regev, *SIAM J. Comput.* **35**, 1070 (2006).
- [3] D. Poulin and P. Wocjan, *Phys. Rev. Lett.* **102**, 130503 (2009).
- [4] R. P. Feynman, *Int. J. Theor. Phys.* **21**, 467 (1982).
- [5] D. Deutsch, *Proc. R. Soc. A* **400**, 97 (1985).
- [6] J. Brooke, D. Bitko, Rosenbaum, and G. Aeppli, *Science* **284**, 779 (1999).
- [7] J. Du, N. Xu, X. Peng, P. Wang, S. Wu, and D. Lu, *Phys. Rev. Lett.* **104**, 030502 (2010).
- [8] J. Preskill, arXiv:1811.10085.
- [9] D. Aharonov, W. Van Dam, J. Kempe, Z. Landau, S. Lloyd, and O. Regev, *SIAM Rev.* **50**, 755 (2008).
- [10] T. Albash and D. A. Lidar, *Rev. Mod. Phys.* **90**, 015002 (2018).
- [11] Y. Subaşı, R. D. Somma, and D. Orsucci, *Phys. Rev. Lett.* **122**, 060504 (2019).
- [12] P. Costa, D. An, Y. R. Sanders, Y. Su, R. Babbush, and D. W. Berry, *PRX Quantum* **3**, 040303 (2022).
- [13] D. An and L. Lin, *ACM Trans. Quantum Comput.* **3**, 1 (2022).
- [14] E. Farhi, J. Goldstone, S. Gutmann, and M. Sipser, arXiv:quant-ph/0001106.
- [15] A. Aspuru-Guzik, A. D. Dutoi, P. J. Love, and M. Head-Gordon, *Science* **309**, 1704 (2005).
- [16] S. P. Jordan, K. S. Lee, and J. Preskill, *Science* **336**, 1130 (2012).
- [17] S. Lee, J. Lee, H. Zhai, Y. Tong, A. M. Dalzell, A. Kumar, P. Helms, J. Gray, Z.-H. Cui, W. Liu *et al.*, *Nat. Commun.* **14**, 1952 (2023).
- [18] L. D. Landau, *Z. Sowjetunion* **2**, 46 (1932).
- [19] C. Zener, *Proc. R. Soc. A* **137**, 696 (1932).
- [20] H. F. Trotter, *Proc. Am. Math. Soc.* **10**, 545 (1959).
- [21] M. Suzuki, *Commun. Math. Phys.* **51**, 183 (1976).
- [22] S. Lloyd, *Science* **273**, 1073 (1996).
- [23] W. Van Dam, M. Mosca, and U. Vazirani, in *Proceedings 42nd IEEE Symposium on Foundations of Computer Science (IEEE, New York, 2001)*, pp. 279–287.
- [24] D. Layden, *Phys. Rev. Lett.* **128**, 210501 (2022).
- [25] M. Steffen, W. van Dam, T. Hogg, G. Breyta, and I. Chuang, *Phys. Rev. Lett.* **90**, 067903 (2003).
- [26] E. Farhi and A. W. Harrow, arXiv:1602.07674.
- [27] L. Zhou, S.-T. Wang, S. Choi, H. Pichler, and M. D. Lukin, *Phys. Rev. X* **10**, 021067 (2020).
- [28] A. M. Childs and Y. Su, *Phys. Rev. Lett.* **123**, 050503 (2019).
- [29] A. M. Childs, Y. Su, M. C. Tran, N. Wiebe, and S. Zhu, *Phys. Rev. X* **11**, 011020 (2021).
- [30] Note that this definition is not unique. The ordering could be reversed in  $U^{(1)}$ , i.e.,  $U_2 U_1$ . While the precise value of the Trotter error will depend on the order, the scaling with  $\delta t$  and  $T$  is independent of this choice.
- [31] M. Suzuki, *J. Math. Phys. (N.Y.)* **26**, 601 (1985).
- [32] Notice that our definition of infidelity differs a bit from the more common  $1 - |\langle \psi | U^\dagger(\infty) U^{(1)}(T) | \psi \rangle|^2$ .

- [33] See Supplemental Material at <http://link.aps.org/supplemental/10.1103/PhysRevLett.131.060602> for proofs of the main theorems, as well as additional technical details and numerical results, which includes Refs. [34–48].
- [34] J. Huyghebaert and H. De Raedt, *J. Phys. A* **23**, 5777 (1990).
- [35] R. Kubo, *J. Phys. Soc. Jpn.* **12**, 570 (1957).
- [36] J. Wurtz and P.J. Love, *Quantum* **6**, 635 (2022).
- [37] M. Kolodrubetz, D. Sels, P. Mehta, and A. Polkovnikov, *Phys. Rep.* **697**, 1 (2017).
- [38] R. F. Stengel, *Optimal Control and Estimation* (Springer, New York, NY, 1994).
- [39] A. P. Peirce, M. A. Dahleh, and H. Rabitz, *Phys. Rev. A* **37**, 4950 (1988).
- [40] N. Khaneja, T. Reiss, C. Kehlet, T. Schulte-Herbrüggen, and S. J. Glaser, *J. Magn. Reson.* **172**, 296 (2005).
- [41] D. M. Reich, M. Ndong, and C. P. Koch, *J. Chem. Phys.* **136**, 104103 (2012).
- [42] T.-S. Ho and H. Rabitz, *Phys. Rev. E* **82**, 026703 (2010).
- [43] L. T. Brady, C. L. Baldwin, A. Bapat, Y. Kharkov, and A. V. Gorshkov, *Phys. Rev. Lett.* **126**, 070505 (2021).
- [44] J. R. McClean *et al.*, *Quantum Sci. Technol.* **5**, 034014 (2020).
- [45] M. Steudtner and S. Wehner, *New J. Phys.* **20**, 063010 (2018).
- [46] A. Tranter, P.J. Love, F. Mintert, and P.V. Coveney, *J. Chem. Theory Comput.* **14**, 5617 (2018).
- [47] O. G. Maupin, A. D. Baczewski, P.J. Love, and A. J. Landahl, *Entropy* **23**, 657 (2021).
- [48] J. D. Whitfield, J. Biamonte, and A. Aspuru-Guzik, *Mol. Phys.* **109**, 735 (2011).
- [49] R. MacKenzie, E. Marcotte, and H. Paquette, *Phys. Rev. A* **73**, 042104 (2006).
- [50] D. Cheung, P. Høyer, and N. Wiebe, *J. Phys. A* **44**, 415302 (2011).
- [51] C. Yi and E. Crosson, [arXiv:2102.12655](https://arxiv.org/abs/2102.12655).
- [52] C. Yi, *Phys. Rev. A* **104**, 052603 (2021).
- [53] B. Şahinoğlu and R. D. Somma, *npj Quantum Inf.* **7**, 119 (2021).
- [54] L. Allen and J. H. Eberly, *Optical Resonance and Two-Level Atoms* (Dover Publications Inc., Mineola, NY, 1987), Vol. 28.
- [55] L. T. Brady, L. Kocia, P. Bienias, A. Bapat, Y. Kharkov, and A. V. Gorshkov, [arXiv:2107.01218](https://arxiv.org/abs/2107.01218).
- [56] M. Honda, E. Itou, Y. Kikuchi, L. Nagano, and T. Okuda, *Phys. Rev. D* **105**, 014504 (2022).
- [57] T. Albash, *Presented at the Quantum Scientific Computing Open User Testbed (QSCOUT) Users Meeting* (2022).
- [58] M. Reiher, N. Wiebe, K. M. Svore, D. Wecker, and M. Troyer, *Proc. Natl. Acad. Sci. U.S.A.* **114**, 7555 (2017).
- [59] Y. Ge, J. Tura, and J. I. Cirac, *J. Math. Phys. (N.Y.)* **60**, 022202 (2019).
- [60] L. Lin and Y. Tong, *Quantum* **4**, 372 (2020).
- [61] K. Wan and I. Kim, [arXiv:2004.04164](https://arxiv.org/abs/2004.04164).
- [62] J. Lemieux, G. Duclos-Cianci, D. Sénéchal, and D. Poulin, *Phys. Rev. A* **103**, 052408 (2021).
- [63] H. Pichler, S.-T. Wang, L. Zhou, S. Choi, and M. D. Lukin, [arXiv:1808.10816](https://arxiv.org/abs/1808.10816).
- [64] G. B. Mbeng, R. Fazio, and G. E. Santoro, [arXiv:1911.12259](https://arxiv.org/abs/1911.12259).
- [65] G. B. Mbeng, R. Fazio, and G. Santoro, [arXiv:1906.08948](https://arxiv.org/abs/1906.08948).
- [66] E. Farhi, J. Goldstone, and S. Gutmann, [arXiv:1411.4028](https://arxiv.org/abs/1411.4028).